ARTICLE

Direct Observation of Gold Nanoparticle Assemblies with the Porin MspA on Mica

Matthew T. Basel,[†] Raj Kumar Dani,[†] Myungshim Kang,[†] Mikhail Pavlenok,[‡] Viktor Chikan,[†] Paul E. Smith,[†] Michael Niederweis,[‡] and Stefan H. Bossmann[†,*]

[†]Department of Chemistry, Kansas State University, Manhattan, Kansas 66506-3701, and [‡]Department of Microbiology, Bevill Biomedical Research Building, Birmingham, The University of Alabama at Birmingham, Birmingham, Alabama 35294-2170

ABSTRACT The octameric porin MspA from *Mycobacterium smegmatis* is sufficiently stable to form a nonmembrane-supported *stand-alone porin* on mica surfaces. About 98% of all MspA octamers were found to stand upright on mica, with their periplasmic loop regions bound to the hydrophilic mica surface. Both, small ($d = 3.7$ nm) and large ($d = 17$ nm) gold nanoparticles bind to MspA, however, in different positions: small gold nanoparticles bind within the MspA pore, whereas the large gold nanoparticles bind to the upper region of MspA. These experiments demonstrate that gold nanoparticles can be positioned at different, well-defined distances from the underlying surface using the MspA pore as a template. These findings represent a significant step toward the use of electrically insulating stable proteins in combination with metal nanoparticles in nanodevices.

KEYWORDS: MspA from *M. smegmatis* · AFM (Magnetic AC Mode) · mica · gold nanoparticle · bio/nanoelectronics

The application of native and bioengineered proteins with dimensions in the nanometer range has been limited because most proteins lose their structural integrity in a non-native environment, impeding their use in technical processes. However, the major channel protein in the outer membrane of *Mycobacterium smegmatis* MspA is an extremely stable protein, retaining its channel structure even after boiling in 3% SDS or extraction with organic solvents.[1] Its physiological function is to enable the exchange of hydrophilic compounds between the environment and the periplasm.[2,3] MspA has the longest membrane-spanning domain of all membrane proteins known to date[4] (Figure 1) and is the only mycobacterial porin that can be purified in milligram quantities.[5]

Another distinct advantage of MspA is its amphiphilic nature. Not only is the interior channel surface much more hydrophilic than its exterior, but the exterior consists of two distinct zones.[4] The crystal structure of MspA has revealed a very hydrophobic "docking region" at the stem of its "goblet", whereas its "rim" section is formed by both hydrophilic and hydrophobic residues. The geometric dimensions of the "docking region" are 3.7 nm in length, and 4.9 nm in diameter.[4] The total length of MspA is 9.6 nm, with a maximal width of 8.8 nm. It is noteworthy that the heptameric channel protein α-hemolsyin[6] also forms a β-barrel protein, but possesses different geometric features compared to MspA.[4] Both channel proteins are water-filled and permeable to cations, anions, and biopolymers. Compared to α-hemolysin, MspA possesses a narrower constriction zone (2.6 *vs* 1.0 nm) and a higher stability.[7] According to results obtained when using surfactant bilayers,[7] organic thiols on gold electrodes,[8,9] water-soluble hydrophobic polymers,[10] highly oriented pyrolytic graphite (HOPG)-surfaces,[10] and bacterial membranes,[10] reconstitution of MspA in various membranes and their artificial models has been observed. Because of its extraordinary stability, MspA has great prospects for future use in nanotechnological applications. Here, we present evidence obtained from atomic force spectroscopy (AFM) demonstrating that MspA is stable on mica surfaces without the support of a membrane, polymer layer, or anything that resembles a hydrophobic membrane. This is of great importance with respect to nanotechnology applications. Furthermore, we show that MspA is able to bind gold nanoparticles (Au NPs) within its funnel shaped hydrophilic channel. This may enable the design and construction of Au@porin assemblies where the Au NPs bind at various well-defined positions within the porin channel.

RESULTS AND DISCUSSION

MspA on Mica. Our aim was to observe and examine the binding of gold nanoparticles to individual MspA pores. The first step

*Address correspondence to sbossman@ksu.edu, mnieder@uab.edu.

Received for review November 19, 2008 and accepted January 24, 2009.

Published online February 4, 2009. 10.1021/nn800786p CCC: $40.75

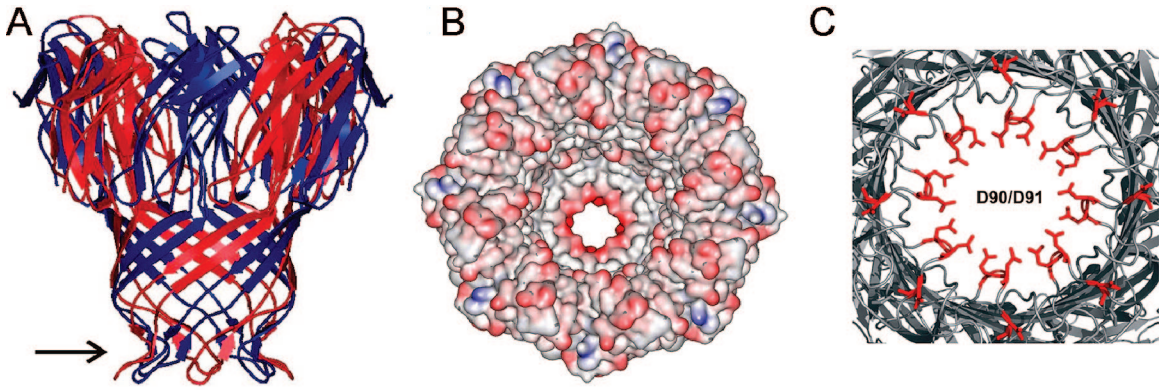

Figure 1. (A) Structure of *M. smegmatis* (side view). The arrow depicts the constriction zone. (B) Electrostatic potential of the hydrophilic channel interior of MspA. Gasteiger charges for the atoms contained in the surface were calculated and visualized using ViewerLite (Accelrys Inc.): red, negative charges; blue, positive charges. (C) Constriction zone formed by aspartates 90 and 91. The coordinates were taken from the crystal structure of MspA (PDB code: 1UUN).[4]

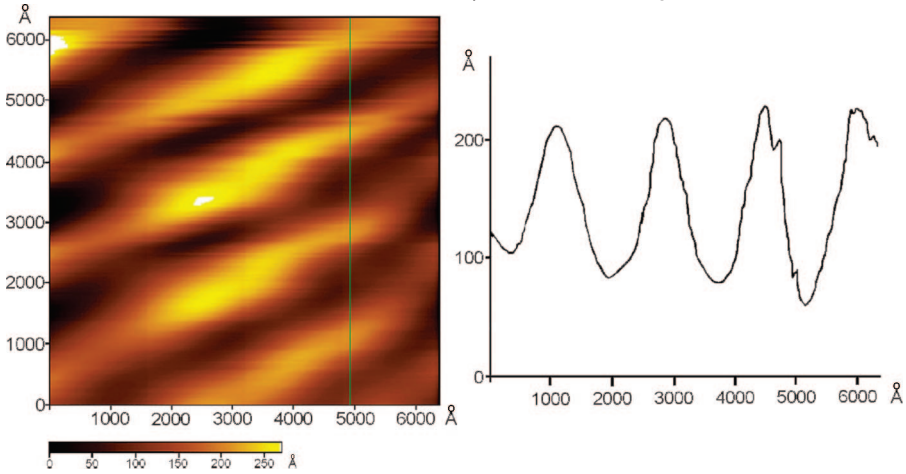

Figure 2. MspA forms a superstructure on mica when deposited from aqueous buffer.

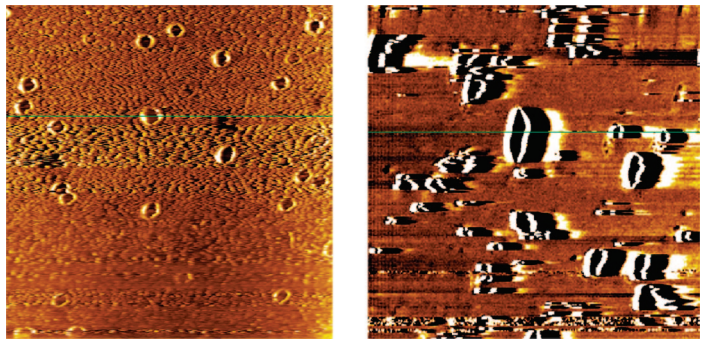

Figure 3. (Left) MspA on mica from MeOH/aqueous buffer (80/20; v/v), image size 200 nm × 200 nm; (right) MspA on mica from MeOH/ aqueous buffer (98/2; v/v), image size 200 nm × 200 nm.

of our study consisted of depositing MspA onto mica from aqueous buffer solution. These structures were then observed by AFM operating in the magnetic A/C mode (MACMode),[11] which uses a magnetically driven oscillating probe with an oscillation amplitude significantly smaller than that of the so-called tapping mode.[12] The result is a superior resolution and less distortion of the sample by AFM imaging. As shown in Figure 2, MspA forms a superstructure on mica that does not exhibit any discernible pores, but rather a wave-like structure. The distance between the maxima is approximately 150 nm with a height difference of 10 nm. This structure appears to be similar to the composition of MspA phases on HOPG that were ob-

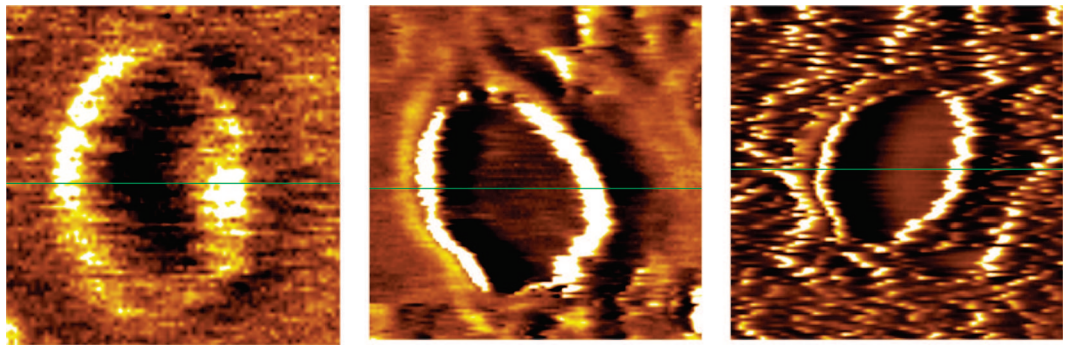

Figure 4. MspA on mica, image size 22 nm × 22 nm: (left) MeOH/ aqueous buffer (40/60; v/v); (middle) MeOH/ aqueous buffer (60/40; v/v); (right) MeOH/ aqueous buffer (98/2; v/v).

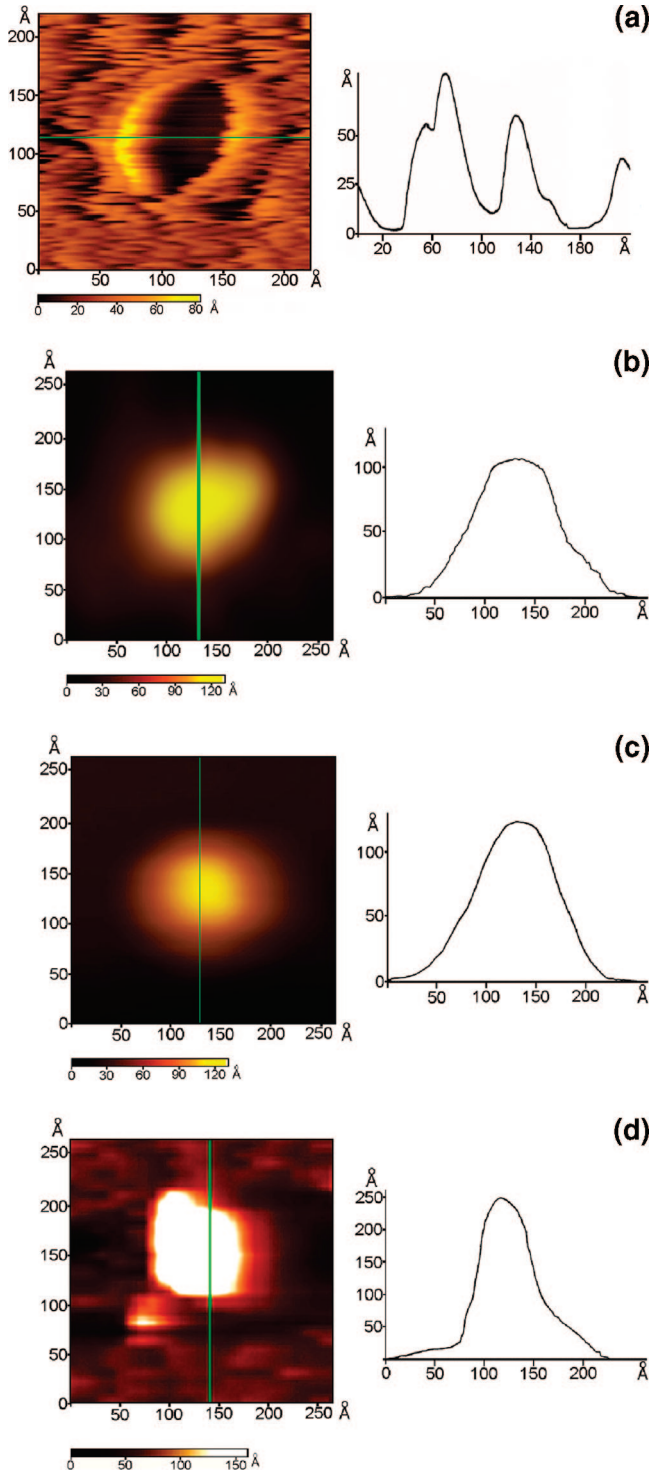

Figure 5. (A) Topology of the MspA homopore, deposited from aqueous buffer (80% MeOH) onto mica, as imaged by AFM (magnetic AC-mode). (B) Topology of the small Au@MspA(126C) assembly, deposited from aqueous buffer (80% MeOH) onto mica, as imaged by AFM (magnetic AC-mode). (C) Topology of the small Au@MspA (wild type, WT) assembly, deposited from aqueous buffer (80% MeOH) onto mica, as imaged by AFM (magnetic AC-mode). (D) Topology of the large Au@MspA(wt) assembly, deposited from aqueous buffer (80% MeOH) onto mica, as imaged by AFM (magnetic AC-mode).

tained previously by the deposition of microdroplets.[13] The observed interaction of individual MspA octamers that form the complex layer structure can be attributed to the hydrophobic interactions of the docking zones[4,14] as well as interprotein hydrogen-bonding.[15]

A series of experiments was performed to obtain single MspA pores on mica. Increasing amounts of methanol (MeOH) were added to the MspA sample to break hydrophobic and hydrogen bonds between individual MspA octamers. With increasing MeOH content, single MspA pores become more and more dominant, until virtually only isolated MspA pores can be observed at 80% MeOH (Figure 3). At higher MeOH concentrations, the octameric MspA begins to deteriorate and various pore sizes and shapes are found.

It is apparent from Figure 4 that single MspA pores can be imaged on mica by using AFM. The strength of the interaction between the MspA monomers is sufficient for MspA to remain an octamer up to a MeOH content of 80%. It must be noted that approximately 98% of the MspA "goblets" appear to stand upright on mica. Their large pore openings are directed outward, whereas the loop region and the constriction zone are directed toward the mica support. Hence, MspA is observed to be stable on mica. When in the MACMode (oscillation frequency: 75 kHz (air)), the oscillating AFM probe conveys a force of approximately 25 pN, which does not distort the protein's structure. Three MspA pores on mica are shown, which were imaged using the AFM's optimal resolution. Deposition from aqueous buffers containing 40, 60, and 80% MeOH did not alter the shape of the pores significantly.

Binding of Gold Nanoparticles Within or on Top of MspA. The presence of open MspA pores in lipid bilayers,[7] monolayers on gold,[8,9] hydrophobic water-soluble polymer layers,[10] and in MspA layers on HOPG[10] has been proven by TEM[10] and electrochemical impedance measurements.[8,9] Recently, we imaged open MspA pores in monolayers of thiol-bound long-chain surfactants on gold by using AFM.[9] The same methodology (AFM in the magnetic AC-mode) has been applied here to image "stand-alone" MspA on mica. The topology plot that was obtained is shown in Figure 5. The dip of more than 5 nm is characteristic for the presence of the inner pore of MspA, although it is not completely accessible to the tip of the AFM, which has a diameter of approximately 7 nm. The height of the outer rim determined by AFM is 10 $\pm$ 1 nm, which is in complete agreement with the dimensions of MspA obtained from the crystal structure.

In a previous study we generated a series of small Au NPs with an average diameter of 3.7 nm, and a series of larger Au NPs with an average diameter of 17 nm.[16] Furthermore, HPLC experiments demonstrated that the binding of both the small and large NPs to MspA in solution occurs with very high binding constants ($K_B > 10^9\ M^{-1}$). Upon binding these Au NPs to the current MspA supported on mica, remarkable changes in the morphology of the Au@MspA assemblies, compared to MspA, can be detected by AFM. The results dif-

fer greatly depending on the diameter of the Au NPs used. Here, the AFM experiments indicate that the inner pore of MspA is no longer accessible to the AFM tip after binding of the small Au NPs. This provided evidence that the binding of the small Au NPs occurs within the inner pore of MspA. Furthermore, the height of the Au@MspA assembly increased to 12.5 ± 0.5 nm, which is about 2 nm higher compared to an empty MspA. In sharp contrast, the binding of the large Au NPs to MspA leads to a significant increase to 26 ±2 nm in the height of the assemblies. This height increase indicates that the large Au NPs bind to the top of the MspA goblet.

The geometrical requirements for Au@MspA complex formation were investigated by a series of calculations performed using the porin octamer coordinates observed in the crystal structure (PDB code: 1UUN),[4] and using the same procedures as our previous study.[16] A gold FCC lattice was constructed using the experimental Au−Au contact distance of 0.288 nm.[17] For the small complex, a spherical Au NP with a diameter of 4 nm (1956 Au atoms) was isolated from the Au lattice. The center of mass of this NP was then moved along the central axis of the porin corresponding to various distances inside the porin. In our previous study, which involved a Q126C mutant of MspA, the NP was predicted to bind inside the porin to facilitate bonding of the Cys residues to the NP. For the wt MspA pore used here, it was observed that small Au NPs also bind with their equator located at the top rim of the MspA goblet. In this case the carboxylate groups of E59 and D134 in extracellular loops[4] provide putative binding sites. For the larger complex, a NP with a diameter of 17 nm (151461 Au atoms) was extracted from the Au lattice and docked directly onto the porin such that no Au atom was located within 0.3 nm of any porin backbone (N, C^{α}, C, O) or C^{β} atom. The resulting complexes and their predicted heights are displayed in Scheme 1. Analysis of the positions of the carboxylate groups of MspA to the postulated Au NP complexes is provided in Table 1. In all the complexes there are carboxylate groups, which could facilitate binding of Au to the porin. The predicted heights are in excellent agreement with the AFM results.

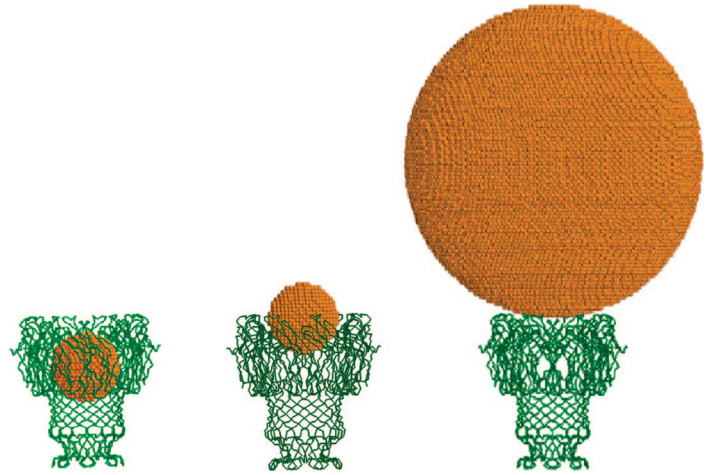

Scheme 1. Calculated heights of the complexes: small Au@MspA^{Q126C} (left, height: 10 nm), small Au@MspA^{WT} (middle, height: 12.5 nm), and large Au@MspA^{WT} complexes (right, height: 26.5 nm).

CONCLUSION

Our AFM measurements have provided evidence that the octameric porin MspA from *Mycobacterium smegmatis* is sufficiently stable to form a nonmembrane-supported stand-alone porin on mica surfaces. The geometric dimensions of the single MspA octamers on mica were identical with those of the crystal structure. Surprisingly, about 98% of all MspA octamers were found to stand upright on mica, with their periplasmic loop regions bound to the hydrophilic mica surface. This binding geometry enables one to study the binding of gold nanoparticles to MspA by AFM. Both, small (d = 3.7 nm) and large (d = 17 nm) gold nanoparticles bind MspA. Depending on the size of the gold nanoparticle, very different binding positions can be discerned: small gold nanoparticles bind within the MspA pore, whereas the large gold nanoparticles bind to the upper region of MspA and are mainly located above the stand-alone porin. Consequently, gold nanoparticles can be bound at well-defined distances from the underlying surface or electrode, respectively. We regard these findings as a significant step toward the use of electrically insulating stable proteins in combination with metal nanoparticles.

TABLE 1. Approximate Distances (nm) from Au Atoms of the NP to Either the C^{γ} of Asp, the C^{δ} of Glu, or the C^{β} of Cys Residues in Each Chain of MspA

MspA	Q126C	wt	wt
NP	Au (d = 4 nm)	Au (d = 4 nm)	Au (d = 17 nm)
D56			0.5
E57			0.4
E59		0.7	0.7
E63	0.9		
Q126C	0.4		
E127	0.8		
D134		0.8	

METHODS

The synthesis and characterization of the small and large nanoparticles is described in another publication of the authors.[16] MspA was harvested from *M. smegmatis* and purified as previously described.[5]

MspA deposition on mica: Stock solutions of MspA (100 mg mL^{-1}) in PS01 buffer[5] were diluted with phosphate buffer (0.050

M, pH = 7.02) to 10 mg mL^{-1}. This solution was then mixed with aliquots of bidistilled H_2O and MeOH. These solutions (1 mg mL^{-1}) were transferred onto freshly cleaved mica by spin-casting (3000 rpm for 120 s) at 298 K. The mica surfaces were then dried under N_2 and imaged by AFM.

Au@MspA deposition on mica: The deposition of Au@MspA on mica was performed as described above at a MeOH content of 80% (v/v). The (small and large) gold nanoparticles ($c = 1 \times 10^{-7}$ M) were mixed with MspA in phosphate buffer and the solution was sonicated for 30s prior to dilution with bidistilled H_2O and MeOH.

AFM imaging: All images using were recorded a PicoScan 2000 AFM (Agilent) in the magnetic A/C-mode (MACmode).[12] MacMode type II tips from Agilent Technologies were used (tip radii < 7 nm, nominal k value $= 2.8$ N/m, resonance frequency $= 50-75$ kHz). The size of the images was corrected according to the results from a calibration procedure using a series of defined tris-homoleptic ruthenium(II)-quaterpyridinium-complexes as model compounds.[18] Typical experimental errors derived from the comparison of similar objects and repetitive imaging of the same object were of the order of 5 relative percent.

Acknowledgment. This publication was made possible by Grant Number P20 RR015563 from the National Center for Research Resources, a component of the National Institutes of Health, and the State of Kansas. Its contents are solely the responsibility of the authors and do not necessarily represent the official view of the NCRR or NIH. S.H.B. and V.C. thank the Terry C. Johnson Center for Basic Cancer Research at Kansas State University for financial support of this study.

REFERENCES AND NOTES

1. Heinz, C.; Roth, E.; Niederweis, M. Purification of Porins from *Mycobacterium smegmatis*. *Methods Mol. Biol.* **2003**, *228*, 139–150.
2. Niederweis, M.; Bossmann, S. H. Nanostructuring at Surfaces Using Proteins. *Encycl. Nanosci. Nanotechnol.* **2004**, 851–867.
3. Engelhardt, H.; Gerbl-Rieger, S.; Krezmar, D.; Schneider-Voss, S.; Engel, A.; Baumeister, W. Structural Properties of the Outer Membrane and the Regular Surface Protein of *Comamonas acidovorans*. *J. Struct. Biol.* **1990**, *105*, 92–102.
4. Faller, M.; Niederweis, M.; Schulz, G. E. The Structure of a Mycobacterial Outer-Membrane Channel. *Science* **2004**, *303*, 1189–1192.
5. Heinz, C.; Niederweis, M. Selective Extraction and Purification of a Mycobacterial Outer Membrane Protein. *Anal. Biochem.* **2000**, *285*, 113–120.
6. Song, L. Z.; Hobough, M. R.; Shustak, M. R.; Cheley, S.; Bayley, H.; Gouaux, J. E. Structure of Staphylococcal alpha-Hemolysin, a Heptameric Transmembrane Pore. *Science* **1996**, *274*, 1859–1866.
7. Engelhardt, H.; Heinz, C.; Niederweis, M. A Tetrameric Porin Limits the Cell Wall Permeability of *Mycobacterium smegmatis*. *J. Biol. Chem.* **2002**, *277*, 37567–37572.
8. Wörner, M.; Niebler, S.; Gogritchiani, E.; Egner, N.; Braun, A. M.; Niederweis, M.; Bossmann, S. H. Nanoarray-Surfaces by Reconstitution of the Porin MspA into Stabilized Long-Chain-Lipid-Monolayers at a Gold-Surface. *Electroanalysis* **2006**, *18*, 1859–1870.
9. Wörner, M.; Lioubashevski, O.; Niebler, S.; Gogritchiani, E.; Egner, N.; Heinz, C.; Hoferer, J.; Cipolloni, M.; Janik, K.; Katz, E.; Braun, A. M.; Willner, I.; Niederweis, M.; Bossmann, S. H. Characterization of Nanostructured-Surfaces Generated by Reconstitution of the Porin MspA from *M. smegmatis* into Stabilized Long-Chain-Monolayers at Gold-Electrodes. *Small* **2007**, *3*, 1084–1097.
10. Bossmann, S. H.; Janik, K.; Pokhrel, M. R.; Heinz, C.; Niederweis, M. Reconstitution of a Porin from *Mycobacterium smegmatis* at HOPG Covered with Hydrophobic Host Layers. *Surf. Interface Anal.* **2004**, *36*, 127–134.
11. Han, W.; Lindsay, S. M.; Jing, T. A Magnetically Driven Oscillating Probe Microscope for Operation in Liquids. *Appl. Phys. Lett.* **1996**, *69*, 4111–4113.
12. Hansma, K. P.; Cleveland, J. P.; Radmacher, M.; Walters, D. A.; Hillner, P. E.; Bezanilla, M.; Fritz, M.; Vie, D.; Hansma, H. G.; Prater, C. B.; *et al*. Tapping Mode Atomic Force Microscopy in Liquids. *Appl. Phys. Lett.* **1994**, *64*, 1738–1740.
13. Niederweis, M.; Heinz, C.; Janik, K.; Bossmann, S. H. Nanostructuring of Carbon Surfaces by Deposition of a Channel-Forming Protein and Subsequent Polymerization of Methyl Methacrylate Prepolymers. *Nano Lett.* **2001**, *1*, 169–174.
14. Stahl, C.; Kubetzko, S.; Kaps, I.; Seeber, S.; Engelhardt, H.; Niederweis, M. MspA Provides the Main Hydrophilic Pathway through the Cell Wall of *Mycobacterium smegmatis*. *Mol. Microbiol.* **2001**, *40*, 451−464 (correction *Mol. Microbiol.* **2005**, *457*, 1509).
15. Niederweis, M.; Ehrt, S.; Heinz, C.; Klčker, U.; Karosi, S.; Swiderek, K. M.; Riley, L.; Benz, R. Cloning of the *MspA* Gene Encoding a Porin from *Mycobacterium smegmatis*. *Mol. Microbiol.* **1999**, *33*, 933–945.
16. Dani, R. K.; Kang, M.; Kalita, M.; Smith, P. E.; Bossmann, S. H.; Chikan, V. MspA Porin-Gold Nanoparticle Assemblies: Enhanced Binding through a Controlled Cysteine Mutation. *Nano Lett.* **2008**, *8*, 1229–1236.
17. De, G.; Rao, C. N. R. Au-Pt Alloy Nanocrystals Incorporated in Silica Films. *J. Mater. Chem.* **2005**, *15*, 891–894.
18. Shi, A.; Pokhrel, M. R.; Bossmann, S. H. Synthesis of Highly Charged Ruthenium(II)-Quaterpyridinium Complexes: A Bottom-Up Approach to Monodisperse Nanostructures. *Synthesis* **2007**, *4*, 505–514.